Equilibrium distributions for relativistic free particles in thermal radiation within classical electrodynamics

Timothy H. Boyer
Department of Physics, The City College of the City University of New York, New York, New York 10031
(Received 13 November 1978)

The equilibrium velocity distribution of classical free particles interacting with random classical radiation is investigated using the model of Einstein and Hopf, and extended to allow relativistic particle velocities. The model considers a massive free particle which has an electric dipole oscillator mounted inside; the oscillator provides the interaction between the particle and the random radiation. In this paper we give the calculations leading to a Fokker-Planck equation for the equilibrium distribution of particle momenta, and evaluate the equation for a number of radiation spectra. We find the following results: (i) If the random classical radiation is the Rayleigh-Jeans law for thermal radiation, then the equilibrium particle distribution follows the Boltzmann distribution only at low temperatures where nonrelativistic particle velocities are involved. The Rayleigh-Jeans law does not lead to the Boltzmann distribution for relativistic free particles. (ii) If the random classical radiation is the zero-point radiation spectrum, then the equilibrium particle distribution is the Lorentz-invariant distribution. (iii) If the random classical radiation is the Planck spectrum with zero-point radiation, then the equilibrium particle distribution goes over asymptotically to the Lorentz-invariant distribution at velocities near the speed of light. Thus no finite number of free particles can form an equilibrium velocity distribution if zero-point radiation is present. The particles will diffuse to velocities ever closer to the speed of light. We conclude that equilibrium for a finite number of particles must involve some explicit mechanism for confinement if classical zero-point radiation is present.

I. INTRODUCTION

The interaction between radiation and matter provides one of the major problems of 20th-century physics, and the ramifications of this problem have led to the creation of quantum theory and quantum electrodynamics. In the present paper we turn to one small aspect of the problem which most physicists regard as already solved. We consider here the equilibrium velocity distributions of classical free particles interacting with random classical radiation. This situation, which lies entirely within classical electrodynamics, was first explored[1,2] over 70 years ago with results confirming conventional expectations. However, the calculations at that time used nonrelativistic particle mechanics. The present paper extends the work to the relativistic domain and finds unexpected results.

The model for the calculations is that provided by Einstein and Hopf[1] in 1910. A massive particle is assumed to contain an electric dipole oscillator which interacts with the random classical radiation. The random radiation causes oscillations of the dipole and hence exerts forces on the massive particle. The particle thus executes a Brownian motion under the influence of the random forces from the random radiation. By appropriate calculations from the electromagnetic forces, it is possible to obtain a Fokker-Planck equation for the distribution of particle momenta in terms of the energy spectrum of the random radiation. The equilibrium particle distributions can be obtained by numerical computation.

In the original work of Einstein and Hopf[1] and of Milne,[2] it is assumed that a finite number of free particles will come to equilibrium with classical thermal radiation, and it is concluded that the Rayleigh-Jeans law leads to the Boltzmann distribution for particle momenta. Both this assumption and conclusion are lost when one treats the particle velocities relativistically. The calculations that follow will instead lead us to these conclusions: (i) The Rayleigh-Jeans law for thermal radiation enforces the Boltzmann distribution for particle momenta in the case of nonrelativistic particle velocities only. For relativistic particle velocities there is an inconsistency between the Rayleigh-Jeans law for thermal radiation and the Boltzmann distribution for free particles. (ii) If the random classical radiation is the zero-point radiation spectrum, then the equilibrium particle distribution is Lorentz invariant. (iii) If the classical radiation spectrum includes zero-point radiation, as, for example, in the Planck spectrum with zero-point radiation, then the equilibrium particle distribution goes over to the Lorentz-invariant distribution for high velocities, and the equilibrium distribution cannot be normalized to a finite number of particles. For any finite number of particles, the random motions will eventually bring the particles to a high velocity, where the thermal radiation at low frequency is not important, and the particle will diffuse out into the divergent high-velocity tail caused by the zero-point radiation at high frequencies. If zero-point radiation is present, then equilibrium for a finite number of particles requires some explicit mechanism for confining the particles.

In the account to follow, we will first discuss the model of Einstein and Hopf, and then carry out the calculations of the random forces for insertion into a Fokker-Planck equation for the distribution of relativistic particle momenta. Once we have obtained the Fokker-Planck equation, we discuss the Rayleigh-Jeans law for thermal radiation and see that it leads to the Boltzmann distribution for free-particle momenta in the nonrelativistic limit, but causes departures from the Boltzmann distribution for relativistic particles. We subsequently discuss the equilibrium particle distributions caused by the Planck law without zero-point radiation, by the zero-point radiation spectrum, and by the Planck spectrum with zero-point radiation.

II. BASIC CALCULATIONS

A. Model of Einstein and Hopf

The particle model used in the present paper is merely an extension to relativistic velocities of that proposed by Einstein and Hopf[1] in 1910 and used again in our work[3] of 1969. A particle of large mass M, constrained to move along the x axis, contains a small electric dipole oscillator $\vec{p}=p\hat{K}$ oriented along the z axis. The dipole oscillator can be pictured crudely as a fixed negative charge $-e$ along with a particle of mass m and charge e at the end of a spring of natural frequency ω_0, giving a damping constant $\Gamma=2e^2/3mc^3$. The charge e, which determines the size of the interaction between the particle and the radiation, may be chosen arbitrarily small and even taken to vanish when the equilibrium particle distribution is established. The magnitude of the charge e determines the time rate at which equilibrium is approached, but does not affect the final equilibrium distribution.

From the Lorentz force on a point charge $\vec{F}=e[\vec{E}+(\vec{v}/c)\times\vec{B}]$ it follows that our oscillating point dipole experiences a force

$$\vec{\mathfrak{F}}'=(\vec{p}'\cdot\nabla')\vec{E}'+c^{-1}\dot{\vec{p}}'\times\vec{B}' \tag{1}$$

when the center of the dipole is at rest, as it is in the rest frame of the massive particle, which we take as the prime frame. In the present case we are interested only in the x component of the force on the dipole, since our massive particle is constrained to move along the x axis.

$$\mathfrak{F}_x'=\frac{\partial E_x'}{\partial z'}\,p'-\frac{1}{c}B_y'\,\frac{dp'}{dt'}\,. \tag{2}$$

In the rest frame of the particle the mechanical motion of the oscillator can be treated accurately with nonrelativistic mechanics, since the velocity of the charge e is given by ω_0 times the displacement of the charge, and we may go to the limit of a point dipole when the displacement vanishes.

The force $\mathfrak{F}_x$ in the laboratory frame can be found from the force $\mathfrak{F}_x'$ in the particle frame by means of a Lorentz transformation. Since the particle is moving with velocity $\vec{v}=c\beta\hat{i}$, we use the Lorentz transformation for the force[4] in the direction of the transformation velocity,

$$\mathfrak{F}_x=\frac{\mathfrak{F}_x'+(v/c^2)\vec{\mathfrak{F}}'\cdot\vec{u}'}{1+vu_x'/c^2}=\mathfrak{F}_x'\,, \tag{3}$$

since $\vec{u}'=0$ is the velocity of the particle in its own rest frame.

For insertion in the Fokker-Planck equation for the distribution of particle momenta, we need the average change and the mean-square change in the particle momentum during a short time interval τ. Since this change of particle momentum is given by the impulse

$$\Delta=\int_{t=t_1}^{t=t_1+\tau}dt\;\mathfrak{F}_x \tag{4}$$

delivered to the particle during the time τ, we need the average impulse $\langle\Delta\rangle=F_x\tau$, where F_x is the average force

$$F_x=\langle\mathfrak{F}_x\rangle\,, \tag{5}$$

and we need the mean-square impulse $\langle\Delta^2\rangle$ delivered to the particle during the time τ,

$$\langle\Delta^2\rangle=\left\langle\left(\int_{t=t_1}^{t=t_1+\tau}dt\;\mathfrak{F}_x\right)^2\right\rangle. \tag{6}$$

The length of time τ is assumed sufficiently long that the oscillator has carried out many oscillations, but sufficiently short that no significant change in the particle velocity will have occurred. By taking the charge e and hence the oscillator damping constant Γ sufficiently small, we can always obtain a suitably long time interval.

The random classical radiation is written in terms of a superposition of plane waves with random phases[5]:

$$\vec{E}(\vec{r},t)=\mathrm{Re}\sum_{\lambda=1}^{2}\int d^3k\,\hat{\epsilon}(\vec{k},\lambda)\mathfrak{h}(\omega_{\vec{k}})\times\exp[i\vec{k}\cdot\vec{r}-i\omega t+i\theta(\vec{k},\lambda)]\,, \tag{7}$$

$$\vec{B}(\vec{r},t)=\mathrm{Re}\sum_{\lambda=1}^{2}\int d^3\hat{k}\,\hat{k}\times\hat{\epsilon}\,\mathfrak{h}(\omega_{\vec{k}})\times\exp[i\vec{k}\cdot\vec{r}-i\omega t+i\theta(\vec{k},\lambda)]\,, \tag{8}$$

where the polarization vectors $\hat{\epsilon}(\vec{k},\lambda)$, $\lambda=1,2$ are orthogonal to $\vec{k}$ and to each other:

$$\hat{\epsilon}(\vec{k},\lambda)\cdot\hat{\epsilon}(\vec{k},\lambda')=\delta_{\lambda\lambda'}\,, \tag{9}$$

$$\vec{k}\cdot\hat{\epsilon}(\vec{k},\lambda)=0\,, \tag{10}$$

$$\sum_{\lambda=1}^{2}\epsilon_i(\vec{k},\lambda)\epsilon_j(\vec{k},\lambda)=\delta_{ij}-\frac{k_ik_j}{k^2}\,, \tag{11}$$

and

$$\pi^2\mathfrak{h}^2(\omega)=g(\omega) \tag{12}$$

corresponds to the electromagnetic energy density per normal mode at frequency ω. The phase $\theta(\vec{k},\lambda)$ is a random variable[5] distributed uniformly on $[0,2\pi]$ and distributed independently for each $\vec{k}$ and λ.

In the rest frame of a particle moving with velocity $\vec{v}=c\beta\hat{i}$ along the x axis, the electromagnetic waves are seen as fields $\vec{E}'(\vec{r}',t')$ and $\vec{B}'(\vec{r}',t')$ obtained from a Lorentz transformation,[6]

$$\vec{E}'(\vec{r}',t')=\mathrm{Re}\sum_{\lambda=1}^{2}\int d^3k\,\{\hat{i}\,\epsilon_x+\hat{j}\gamma[\epsilon_y-\beta(\hat{k}\times\hat{\epsilon})_z] +\hat{K}\gamma[\epsilon_z+\beta(\hat{k}\times\hat{\epsilon})_y]\}\,\mathfrak{h}(\omega_{\vec{k}}) \times\exp[i\vec{k}'\cdot\vec{r}'-i\omega't'+i\theta(\vec{k},\lambda)]\,, \tag{13}$$

$$\vec{B}'(\vec{r}',t')=\mathrm{Re}\sum_{\lambda=1}^{2}\int d^3k\,\{\hat{i}(\hat{k}\times\hat{\epsilon})_x+\hat{j}\gamma[(\hat{k}\times\hat{\epsilon})_y+\beta\epsilon_z] +\hat{K}\gamma[(\hat{k}\times\hat{\epsilon})_z-\beta\epsilon_y]\}\,\mathfrak{h}(\omega_{\vec{k}}) \times\exp[i\vec{k}'\cdot\vec{r}'-i\omega't'+i\theta(\vec{k},\lambda)]\,. \tag{14}$$

The connection between the primed and unprimed variable is the standard Lorentz transformation,[7] including the frequency and wave vector[8]

$$k'=\gamma(k-\beta k_x),\quad k_x'=\gamma(k_x-\beta k),\quad k_y'=k_y,\quad k_z'=k_z\,, \tag{15}$$

where $\omega=ck$ and $\gamma=(1-\beta^2)^{-1/2}$.

The dipole oriented along the z direction oscillates with simple harmonic motion in the particle rest frame while driven by the electric field $E_z'(0,t')$ and damped by the radiation reaction force,[9]

$$\frac{d^2p'}{dt'^2}+\omega_0^2p'-\Gamma\frac{d^3p'}{dt'^3}=\tfrac{3}{2}\Gamma c^3E_z'(0,t')\,, \tag{16}$$

where we have placed the oscillator at the origin of the primed coordinate system. The combination $\frac{3}{2}\Gamma c^3$ corresponds to e^2/m in the crude picture of the oscillator as a charged particle on the end of a spring; for convenience we will write

$$\tfrac{3}{2}\Gamma c^3=e^2/m=b\,. \tag{17}$$

If we substitute Eq. (13) for the random radiation field $E_x'(0',t')$ into the equation of motion (16), we find the steady-state motion of the oscillator,

$$p'=\mathrm{Re}\sum_{\lambda=1}^{2}\int d^3k\,b\,C^{-1}(\omega')\gamma[\epsilon_z+\beta(\hat{k}\times\hat{\epsilon})_y]\mathfrak{h}(\omega) \times\exp[-i\omega't'+i\theta(\vec{k},\lambda)]\,, \tag{18}$$

where

$$C(\omega')=-\omega'^2+\omega_0^2-i\Gamma\omega'^3\,. \tag{19}$$

B. Calculation of the average force F_x

The fluctuating force $\mathfrak{F}_x'$ on the particle in the particle rest frame can be obtained from Eqs. (2), (13), (14), and (18). Transforming the force back to the lab frame with Eq. (3), we have

$$\begin{aligned}\mathfrak{F}_x=&\,\mathrm{Re}\sum_{\lambda_1=1}^{2}\int d^3k_1\,\epsilon_{1x}\,ik_{1z}'\,\mathfrak{h}(\omega_1)\exp[-i\omega_1't'+i\theta(\vec{k}_1,\lambda_1)]\\ &\times\mathrm{Re}\sum_{\lambda_2=1}^{2}\int d^3k_2\,b\,C^{-1}(\omega_2')\gamma[\epsilon_{2z}+\beta(\hat{k}_2\times\hat{\epsilon}_2)_y]\mathfrak{h}(\omega_2)\exp[-i\omega_2't'+i\theta(\vec{k}_2,\lambda_2)]\\ &-c^{-1}\mathrm{Re}\sum_{\lambda_1=1}^{2}\int d^3k_1\,\gamma[(\hat{k}_1\times\hat{\epsilon}_1)_y+\beta\epsilon_{1z}]\mathfrak{h}(\omega_1)\exp[-i\omega_1't'+i\theta(\vec{k}_1,\lambda_1)]\\ &\times\mathrm{Re}\sum_{\lambda_2=1}^{2}\int d^3k_2\,b\,C^{-1}(\omega_2')\gamma[\epsilon_{2z}+\beta(\hat{k}_2\times\hat{\epsilon}_2)_y](-i\omega_2')\mathfrak{h}(\omega_2)\exp[-i\omega_2't'+i\theta(\vec{k}_2,\lambda_2)]\,.\end{aligned} \tag{20}$$

To find the average force $F_x=\langle\mathfrak{F}_x\rangle$, we carry out the average over the random phases $\theta(\vec{k},\lambda)$,

$$\begin{aligned}&\langle\exp[i\theta(\vec{k}_1,\lambda_1)]\exp[-i\theta(\vec{k}_2,\lambda_2)]\rangle=\delta_{\lambda_1\lambda_2}\delta^3(\vec{k}_1-\vec{k}_2)\\ &\langle\exp[i\theta(\vec{k}_1,\lambda_1)]\exp[i\theta(\vec{k}_2,\lambda_2)]\rangle=0\,.\end{aligned} \tag{21}$$

Then integrating and summing over the δ functions we find,

$$F_x=\frac{1}{2}\sum_{\lambda=1}^{2}\int d^3k\,\{\epsilon_x\gamma[\epsilon_z+\beta(\hat{k}\times\hat{\epsilon})_y]k_z'\Gamma\omega'^3b\,|C(\omega')|^{-2}\mathfrak{h}^2(\omega)$$
$$-c^{-1}\gamma[(\hat{k}\times\hat{\epsilon})_y+\beta\epsilon_z]\gamma[\epsilon_z+\beta(\hat{k}\times\hat{\epsilon})_y]\Gamma\omega'^4b\,|C(\omega')|^{-2}\mathfrak{h}^2(\omega)\}, \tag{22}$$

where, as always, the primed and unprimed variables are connected by the Lorentz transformation as in (15).

Now using Eq. (11), we carry out the sum over the polarizations

$$\sum_{\lambda=1}^{2}\epsilon_x\epsilon_z=-\frac{k_xk_z}{k^2},\quad \sum_{\lambda=1}^{2}\epsilon_z\epsilon_z=1-\frac{k_z^2}{k^2},$$
$$\sum_{\lambda=1}^{2}\epsilon_x(\hat{k}\times\hat{\epsilon})_y=\frac{k_z}{k},\quad \sum_{\lambda=1}^{2}\epsilon_z(\hat{k}\times\hat{\epsilon})_y=-\frac{k_x}{k}, \tag{23}$$
$$\sum_{\lambda=1}^{2}(\hat{k}\times\hat{\epsilon})_y(\hat{k}\times\hat{\epsilon})_y=1-\frac{k_y^2}{k^2}.$$

Furthermore, we can change the variable of integration over to d^3k' by using the Jacobian of the transformation in Eqs. (15),

$$d^3k=d^3k'\,\gamma(k'+\beta k_x')/k'. \tag{24}$$

Inserting Eqs. (23) and (24) into (22), we find

$$F_x=\frac{1}{2}\int d^3k'\,\gamma(k'+\beta k_x')b\Gamma c^3k'^2\,|C(\omega')|^{-2}\mathfrak{h}^2(\omega)$$
$$\times k^{-2}\{\gamma k_z'[k_z(\beta k-k_x)]$$
$$-\gamma^2k'[\beta k^2+\beta k_x^2-(1+\beta^2)k_xk]\}. \tag{25}$$

At this point Eq. (15) is used to eliminate all unprimed variables. When the expression is simplified, the force becomes

$$F_x=\frac{1}{2}\int d^3k'\,\frac{b\Gamma c^3k'^2}{|C(\omega')|^2}\left(\frac{\mathfrak{h}^2(\gamma(\omega'+\beta ck_x'))}{\gamma(k'+\beta k_x')}\right)$$
$$\times k_x'(k'^2-k_z'^2). \tag{26}$$

Since the variable of integration is a dummy variable, we may now drop all the primes.

Next we change to spherical polar coordinates choosing the x axis as the polar axis, $k_x=k\cos\theta$. The integration in ϕ may be carried out easily and the integration in θ changed to one in the dummy variable $X=\cos\theta$. We find

$$F_x=\frac{1}{2}\int_0^\infty d\omega\int_{-1}^{1}dX\,\frac{b\Gamma\omega^7}{c^4|C(\omega)|^2}\left(\frac{\mathfrak{h}^2(\omega\gamma(1+\beta X))}{\omega\gamma(1+\beta X)}\right)$$
$$\times\pi X(1+X^2). \tag{27}$$

The dipole oscillator p' responds mainly to radiation at its natural frequency $\omega'=\omega_0$. As the charge e and hence damping constant Γ becomes smaller, it requires a longer time for the oscillator to give a fixed size response to a fixed incident wave, and hence phase coherence between the oscillator and the random radiation is limited to a narrower range of frequencies. In the narrow-linewidth limit we have[10]

$$\lim_{e^2/m\to 0}(e^2/m)|C(\omega)|^{-2}$$
$$=(\tfrac{3}{4}\pi c^3/\omega_0^4)[\delta(\omega-\omega_0)+\delta(\omega+\omega_0)], \tag{28}$$

where here $b=e^2/m$. Introducing this narrow-linewidth limit into (27), and carrying out the integration over ω, we have

$$F_x=\frac{3}{8}\frac{\Gamma\omega_0^3}{c}\int_{-1}^{1}dX\,X(1+X^2)\,\frac{g(\omega_0\gamma(1+\beta X))}{\omega_0\gamma(1+\beta X)}, \tag{29}$$

where $g(\omega)=\pi^2\mathfrak{h}^2(\omega)$ from (12) is the energy per normal mode.

There are two easily available checks on expression (29) for the average force F_x. The first involves the zero-point radiation spectrum $g(\omega)=\frac{1}{2}\hbar\omega$. In this case it is easy to see that the integrand in (29) becomes simply $\frac{1}{2}\hbar X(1+X^2)$, which, as an odd function of X, vanishes on integration from -1 to $+1$, giving $F_x=0$. This is as it should be; zero-point radiation is a Lorentz-invariant spectrum,[11] and hence no velocity-dependent forces are possible.

The second check involves the nonrelativistic limit which was calculated originally by Einstein and Hopf,[1] and also given in our work[3] of 1969. If we retain terms only through first order in β, we have from a Taylor series expansion

$$F_x\cong\frac{3}{8}\frac{\Gamma\omega_0^3}{c}\int_{-1}^{1}dX\,\frac{X(1+X^2)}{\omega_0}\left(g(\omega_0)(1-\beta X)+\omega_0\beta X\frac{dg(\omega_0)}{d\omega_0}\right)$$
$$\cong-\frac{2}{5}\frac{\Gamma\omega_0^2}{c}\,\beta\left(g(\omega_0)-\frac{dg}{d\omega_0}\right). \tag{30}$$

If we recall the connection between the spectral energy density $\rho(\omega)$ and the energy per normal mode $g(\omega)$,

$$\rho(\omega)=(\omega^2/\pi^2c^3)g(\omega), \tag{31}$$

we see that (30) is in exact agreement with the earlier nonrelativistic expression.[12]

C. Calculation of the mean-square impulse $\langle\Delta^2\rangle$

The fluctuating impulse Δ follows from the fluctuating force $\mathfrak{F}_x$ as in Eq. (4). Now the time t' for the action of a force on the massive particle corresponds to the time in the rest frame of the particle, and thus involves a proper time interval with

$$t'=t/\gamma . \tag{32}$$

Hence from (3) and (32) we can rewrite the impulse (4) delivered to the particle during time τ as

$$\Delta=\int_{t_1}^{t_1+\tau}\mathfrak{F}_x\,dt=\int_{t_1'}^{t_1'+\tau/\gamma}\mathfrak{F}_x'\gamma\,dt' =\gamma\int_{t_1'}^{t_1'+\tau/\gamma}\left(\frac{\partial E_x'}{\partial z'}p'-\frac{1}{c}B_y'\frac{dp'}{dt'}\right)dt' . \tag{33}$$

We can integrate the second term of the last line of (33) by parts to obtain

$$\int_{t_1'}^{t_1'+\tau/\gamma}B_y'\frac{dp'}{dt'}dt'=[B_y'p']_{t_1'}^{t_1'+\tau/\gamma}-\int_{t_1'}^{t_1'+\tau/\gamma}\frac{\partial B_y'}{\partial t'}p'\,dt' , \tag{34}$$

and then neglect the evaluated end-point term in brackets since it does not depend upon the length of time τ. Next we use the y component of Maxwell's equation,

$$\nabla'\times\vec{E}'=-c^{-1}\frac{\partial\vec{B}'}{\partial t'} , \tag{35}$$

to give

$$\Delta=\gamma\int_{t_1'}^{t_1'+\tau/\gamma}\left[\frac{\partial E_x'}{\partial z'}p'-\left(\frac{\partial E_x'}{\partial z'}-\frac{\partial E_z'}{\partial x'}\right)p'\right]dt' =\gamma\int_{t_1'}^{t_1'+\tau/\gamma}\frac{\partial E_z'}{\partial x'}p'\,dt' . \tag{36}$$

We now introduce the explicit forms for $\partial E_z'(0,t')/\partial x'$ and p' from Eqs. (13) and (18) to obtain

$$\Delta=\gamma\int_{t_1'}^{t_1'+\tau/\gamma}dt'\,\mathrm{Re}\sum_{\lambda_1=1}^{2}\int d^3k_1\,\gamma[\epsilon_{1z}+\beta(\hat{k}_1\times\hat{\epsilon}_1)_y]\,ik_{1x}'\mathfrak{h}(\omega_1)\exp[-i\omega_1't'+i\theta(\vec{k}_1,\lambda_1)] \times\mathrm{Re}\sum_{\lambda_2=1}^{2}\int d^3k_2\,bC^{-1}(\omega_2')\gamma[\epsilon_{2z}+\beta(\hat{k}_2\times\hat{\epsilon}_2)_y]\mathfrak{h}(\omega_2)\exp[-i\omega_2't'+i\theta(\vec{k}_2,\lambda_2)] . \tag{37}$$

For convenience in later manipulations we will introduce the notations

$$A_1=\exp\{-i[\mu_1\omega_1't'-\mu_1\theta(\vec{k}_1,\lambda_1)]\} , \tag{38}$$

$$C(\mu_1\omega_1')=-(\mu_1\omega_1')^2+\omega_0^2-i\Gamma(\mu_1\omega_1')^3 , \tag{39}$$

where $\mu_1=\pm1$ is a parameter in a summation to take the real part, so that Eq. (37) becomes

$$\Delta=\gamma\int_{t_1'}^{t_1'+\tau/\gamma}dt'\frac{1}{2}\sum_{\mu_1}\sum_{\lambda_1=1}^{2}\int d^3k_1\,\gamma[\epsilon_{1z}+\beta(\hat{k}_1\times\hat{\epsilon}_1)_y]i\mu_1k_{1x}'\mathfrak{h}(\omega_1)A_1 \times\frac{1}{2}\sum_{\mu_2}\sum_{\lambda_2=1}^{2}\int d^3k_2\,bC^{-1}(\mu_2\omega_2')\gamma[\epsilon_{2z}+\beta(\hat{k}_2\times\hat{\epsilon}_2)_y]\mathfrak{h}(\omega_2)A_2 . \tag{40}$$

The time dependence is entirely contained in A_1 and A_2 so that the time integral becomes

$$\int_{t_1'}^{t_1'+\tau/\gamma}dt'A_1A_2=\frac{i\{\exp[-i(\mu_1\omega_1'+\mu_2\omega_2')\tau/\gamma]-1\}}{\mu_1\omega_1'+\mu_2\omega_2'}\exp\{-i[(\mu_1\omega_1'+\mu_2\omega_2')t_1'-(\mu_1\theta_1+\mu_2\theta_2)]\} . \tag{41}$$

Next we square the expression, giving

$$\Delta^2=\frac{\gamma^2}{16}\sum_{\mu_1}\cdots\sum_{\mu_4}\sum_{\lambda_1}\cdots\sum_{\lambda_4}\int d^3k_1\cdots\int d^3k_4\,\gamma^4[\epsilon_{1z}+\beta(\hat{k}_1\times\hat{\epsilon}_1)_y][\epsilon_{2z}+\beta(\hat{k}_2\times\hat{\epsilon}_2)_y][\epsilon_{3z}+\beta(\hat{k}_3\times\hat{\epsilon}_3)_y][\epsilon_{4z}+\beta(\hat{k}_4\times\hat{\epsilon}_4)_y] \times i\mu_1k_{1x}'i\mu_3k_{3x}'bC^{-1}(\mu_2\omega_2')bC^{-1}(\mu_4\omega_4')\mathfrak{h}_1\mathfrak{h}_2\mathfrak{h}_3\mathfrak{h}_4 \times\frac{i\{\exp[-i(\mu_1\omega_1'+\mu_2\omega_2')\tau/\gamma]-1\}}{\mu_1\omega_1'+\mu_2\omega_2'}\frac{i\{\exp[-i(\mu_3\omega_3'+\mu_4\omega_4')\tau/\gamma]-1\}}{\mu_3\omega_3'+\mu_4\omega_4'} \times\exp\{-i[(\mu_1\omega_1'+\mu_2\omega_2'+\mu_3\omega_3'+\mu_4\omega_4')t_1'-(\mu_1\theta_1+\mu_2\theta_2+\mu_3\theta_3+\mu_4\theta_4)]\} . \tag{42}$$

We now average over the random phases:

$$\langle \exp[i(\mu_1\theta_1 + \mu_2\theta_2 + \mu_3\theta_3 + \mu_4\theta_4)]\rangle = \delta_{(1)(-2)}\delta_{(3)(-4)} + \delta_{(1)(-3)}\delta_{(2)(-4)} + \delta_{(1)(-4)}\delta_{(2)(-3)}, \tag{43}$$

where $\delta_{(1)(-2)}$ stands for

$$\delta_{(1)(-2)} = \delta_{\mu_1 - \mu_2}\delta_{\lambda_1\lambda_2}\delta^3(\vec{k}_1 - \vec{k}_2). \tag{44}$$

The dependence of Δ^2 upon the starting time t_1 is seen to vanish upon averaging. After summing and integrating over the δ functions, we find

$$\begin{aligned}\langle \Delta^2\rangle = \frac{\gamma^2}{16}\sum_{\mu_1}\sum_{\mu_2}\sum_{\lambda_1}\sum_{\lambda_2}\int d^3k_1\int d^3k_2\,\gamma^4[\epsilon_{1z} + \beta(\hat{k}_1\times\hat{\epsilon}_1)_y]^2[\epsilon_{2z} + \beta(\hat{k}_2\times\hat{\epsilon}_2)_y]^2 \mathfrak{h}_1^2\mathfrak{h}_2^2 \\ \times\Bigg\{ -\mu_1 k'_{1x}\mu_2 k'_{2x} bC^{-1}(\mu_1\omega'_1) bC^{-1}(\mu_2\omega'_2)\tau^2\gamma^{-2} \\ + k'^2_{1x}\frac{b^2}{|C(\omega'_2)|^2}\frac{|\exp[-i(\mu_1\omega'_1 + \mu_2\omega'_2)\tau/\gamma] - 1|^2}{(\mu_1\omega'_1 + \mu_2\omega'_2)^2} \\ + \mu_1 k'_{1x}\mu_2 k'_{2x}\frac{b}{C(-\mu_1\omega'_1)}\frac{b}{C(\mu_2\omega'_2)}\frac{|\exp[-i(\mu_1\omega'_1 + \mu_2\omega'_2)\tau/\gamma] - 1|^2}{(\mu_1\omega'_1 + \mu_2\omega'_2)^2}\Bigg\},\end{aligned} \tag{45}$$

where we note that $C(-\mu\omega') = C^*(\mu\omega')$, and where we have set

$$\frac{\exp[-i(\mu_1\omega'_1 + \mu_2\omega'_2)\tau/\gamma] - 1}{\mu_1\omega'_1 + \mu_2\omega'_2}\delta_{\mu_1 - \mu_2}\delta^3(\vec{k}_1 - \vec{k}_2) = -i\left(\frac{\tau}{\gamma}\right)\delta_{\mu_1 - \mu_2}\delta^3(\vec{k}_1 - \vec{k}_2). \tag{46}$$

Now the first term for $\langle\Delta^2\rangle$ in Eq. (45) involving the factor τ^2 is just $(F_x\tau)^2$, where F_x is the average force given in Eq. (29). In the present case we have F_x in the form

$$F_x = \frac{1}{4}\sum_{\mu}\sum_{\lambda=1}^{2}\int d^3k\,\gamma^2[\epsilon_x + \beta(\hat{k}\times\hat{\epsilon})_y]^2\mathfrak{h}^2 \times i\mu k'_x bC^{-1}(\mu\omega'). \tag{47}$$

The sum over μ gives $C^{-1}(\omega') - C^{-1}(-\omega') = 2i\Gamma\omega'^3/|C(\omega')|^2$. Introducing the sum over polarizations as in Eq. (23) and changing to the prime variables as in Eqs. (15) and (24), we arrive at exactly our earlier expression for F_x given in Eq. (26).

The last term for $\langle\Delta^2\rangle$ in Eq. (45) includes the factors $bC^{-1}(-\mu_1\omega'_1)bC^{-1}(\mu_2\omega'_2)$. It is second order in the oscillator damping constant Γ and hence negligible compared to the middle term in (45). This higher-order behavior can be seen from the fact that the real part of $C^{-1}(-\mu_1\omega'_1)$ changes sign as ω'_1 passes through ω_0, so that there is a cancellation between the large plus and minus contributions, as there is not for $|C(\mu_1\omega'_1)|^2$, which is always positive. Another way to see this higher-order behavior is to convert the expression $bC^{-1}(-\mu_1\omega'_1)$ to the form

$$\begin{aligned} bC^{-1}(-\mu_1\omega'_1) &= bC(\mu_1\omega'_1)/|C(\omega'_1)|^2 \\ &\sim (3\pi c^3/4\omega_0^4)[(-\omega'^2_1 + \omega_0^2) - i\Gamma(\mu_1\omega'_1)^3]\delta(\omega'_1 - \omega_0) \\ &= (3\pi c^3/4\omega_0^4)[-i\Gamma(\mu_1\omega_0)^3]\delta(\omega'_1 - \omega_0),\end{aligned}$$

where the δ-function behavior follows from the narrow-linewidth approximation in Eq. (28). The expression $bC^{-1}(\mu_2\omega'_2)$ can be converted in the same manner giving the second factor of Γ.

The middle term for $\langle\Delta^2\rangle$ in Eq. (45) is linear in both Γ and τ, and will be designated by $\langle\Delta_\delta^2\rangle$ so that

$$\begin{aligned}\langle\Delta_\delta^2\rangle &= \langle\Delta^2\rangle - (F_x\tau)^2 + O(\Gamma^2) \\ &= \langle\Delta^2\rangle - \langle\Delta\rangle^2 + O(\Gamma^2) \\ &= \frac{\gamma^2}{16}\sum_{\mu_1}\sum_{\mu_2}\sum_{\lambda_1}\sum_{\lambda_2}\int d^3k_1\int d^3k_2\,\gamma^4[\epsilon_{1z} + \beta(\hat{k}_1\times\hat{\epsilon}_1)_y]^2[\epsilon_{2z} + \beta(\hat{k}_2\times\hat{\epsilon}_2)_y]^2 \\ &\quad\times\mathfrak{h}_1^2\mathfrak{h}_2^2 k'^2_{1x}\frac{b^2}{|C(\omega'_2)|^2}\frac{|\exp[-i(\mu_1\omega'_1 + \mu_2\omega'_2)\tau/\gamma] - 1|^2}{(\mu_1\omega'_1 + \mu_2\omega'_2)^2}.\end{aligned} \tag{48}$$

The dependence upon the parameters μ_1 and μ_2 is contained entirely in the last factor, which can be rewritten as

$$\sum_{\mu_1}\sum_{\mu_2}\frac{|\exp[-i(\mu_1\omega_1'+\mu_2\omega_2')\tau/\gamma]-1|^2}{(\mu_1\omega_1'+\mu_2\omega_2')^2}=8\left[\frac{1}{(\omega_1'+\omega_2')^2}\sin^2\left(\frac{\omega_1'+\omega_2'}{2}\frac{\tau}{\gamma}\right)+\frac{1}{(\omega_2'-\omega_1')^2}\sin^2\left(\frac{\omega_2'-\omega_1'}{2}\frac{\tau}{\gamma}\right)\right]. \tag{49}$$

The needed sums over the polarizations appear in the Eqs. (23). We also change the variables of integration over to the prime variables of the particles's rest frame using (15) and (24). We obtain from (48):

$$\begin{aligned}\langle\Delta_\delta^2\rangle=\frac{\gamma^2}{2}\int d^3k_1'\int d^3k_2'\,\gamma\left(1+\frac{\beta k_{1x}'}{k_1'}\right)\gamma\left(1+\frac{\beta k_{2x}'}{k_2'}\right)\gamma^2[\gamma^2(k_1'+\beta k_{1x}')]^{-2}(k_1'^2-k_{1z}'^2)k_{1x}'^2\mathfrak{h}^2(\gamma(\omega_1'+\beta c k_{1x}'))\\ \times b^2|C(\omega_2')|^{-2}\gamma^2[\gamma^2(k_2'+\beta k_{2x}')]^{-2}(k_2'^2-k_{2z}'^2)\mathfrak{h}^2(\gamma(\omega_2'+\beta c k_{2x}'))\\ \times\{(\omega_1'+\omega_2')^{-2}\sin^2[\tfrac{1}{2}(\omega_1'+\omega_2')\tau/\gamma]+(\omega_2'-\omega_1')^{-2}\sin^2[\tfrac{1}{2}(\omega_2'-\omega_1')\tau/\gamma]\}.\end{aligned} \tag{50}$$

At this point we may drop the primes on the variables of integration and introduce spherical polar coordinates with the x axis as the polar axis. The integrations in ϕ_1 and ϕ_2 are easily carried out, and the integrations in θ_1 and θ_2 can be changed over to integrations in the dummy variables $X=\cos\theta_1$, $Y=\cos\theta_2$. Expression (50) for $\langle\Delta_\delta^2\rangle$ then becomes

$$\begin{aligned}\langle\Delta_\delta^2\rangle=\frac{\gamma^2}{2}\int_0^\infty dk_1k_1^2 2\pi\int_{-1}^1 dX\int_0^\infty dk_2k_2^2 2\pi\int_{-1}^1 dY\frac{1}{k_1k_2}\,k_1^2\frac{1+X^2}{2}\,k_1^2X^2\frac{\mathfrak{h}^2(\omega_1\gamma(1+\beta X))}{k_1\gamma(1+\beta X)}\frac{b^2}{|C(\omega_2)|^2}\\ \times k_2^2\frac{(1+Y^2)}{2}\frac{\mathfrak{h}^2(\omega_2\gamma(1+\beta Y))}{k_2\gamma(1+\beta Y)}\\ \times\left[\frac{1}{(\omega_1+\omega_2)^2}\sin^2\left(\frac{\omega_1+\omega_2}{2}\frac{\tau}{\gamma}\right)+\frac{1}{(\omega_2-\omega_1)^2}\sin^2\left(\frac{\omega_2-\omega_1}{2}\frac{\tau}{\gamma}\right)\right].\end{aligned} \tag{51}$$

Now we go to the limit of times τ long compared to the characteristic frequency ω_0 of the oscillator. In this case, the term in $\omega_1+\omega_2$ remains small while the term in $\omega_2-\omega_1$ is sharply peaked at $\omega_2-\omega_1=0$. Also in the narrow-linewidth approximation, $|C(\omega_2)|^{-2}$ gives a sharp peak at $\omega_2=\omega_0$. Hence we first integrate with respect to $\omega_1=ck_1$, changing the variable to $u=\omega_1-\omega_2$, extending the lower limit of integration to $-\infty$, and using

$$\int_{-\infty}^\infty\frac{\sin^2\tau u}{u^2}du=\pi\tau. \tag{52}$$

Thus all factors of ω_1 not appearing in the combination $\omega_1-\omega_2$ are replaced by the value ω_2. Next we integrate with respect to ω_2 while assuming the narrow-linewidth limit for the oscillator as given in (28). This changes all factors of ω_2 not appearing in $|C(\omega_2)|^{-2}$ over to ω_0. Finally, introducing $g(\omega)=\pi^2\mathfrak{h}^2(\omega)$ and $\Gamma=2b/3c^3$ from (12) and (17), we obtain our result

$$\begin{aligned}\langle\Delta_\delta^2\rangle=\gamma\frac{9}{32}\frac{\Gamma\omega_0^4}{c^2}\tau\\ \times\int_{-1}^1 dX\,X^2(1+X^2)\left(\frac{g(\omega_0\gamma(1+\beta X))}{\omega_0\gamma(1+\beta X)}\right)\\ \times\int_{-1}^1 dY(1+Y^2)\left(\frac{g(\omega_0\gamma(1+\beta Y))}{\omega_0\gamma(1+\beta Y)}\right).\end{aligned} \tag{53}$$

The same two checks on our result that were available earlier for F_x are also possible here. In the case of zero-point radiation, $g(\omega)=\frac{1}{2}\hbar\omega$, the integrations in X and Y collapse to

$$\int dX\,X^2(1+X^2)\int dY(1+Y^2),$$

giving $\langle\Delta_\delta^2\rangle=\text{const}\gamma\tau$. We will see in Sec. IIID that this is precisely the form which leads to a Lorentz-invariant particle distribution, as physically it should since the zero-point spectrum is Lorentz invariant. The nonrelativistic limit corresponds to evaluating $\langle\Delta_6^2\rangle$ for the particle at rest, $\beta=0$,

$$\langle\Delta_6^2(0)\rangle=\frac{9}{32}\frac{\Gamma\omega_0^4}{c^2}\tau\int_{-1}^{1}dX X^2(1+X^2)\frac{g(\omega_0)}{\omega_0}\times\int_{-1}^{1}dY(1+Y^2)\frac{g(\omega_0)}{\omega_0}\;. \tag{54}$$

In this case the integrals in X and Y are again elementary, and the result for $\langle\Delta_6^2(0)\rangle$ agrees exactly with the nonrelativistic result published earlier,[13]

$$\langle\Delta_6^2(0)\rangle=\tfrac{4}{5}(\Gamma\omega_0^2/c^2)\tau g^2(\omega_0)\,, \tag{55}$$

when we make the connection between $g(\omega_0)$ and $\rho(\omega_0)$ given in (31).

D. Fokker-Planck equation for momentum distribution

The Fokker-Planck equation for the distribution of particle momentum in equilibrium is of the form[14]

$$-P(p)F_x\tau+\frac{1}{2}\frac{\partial}{\partial p}(P(p)\langle\Delta_6^2\rangle)=0\,, \tag{56}$$

where $P(p)dp$ is the number of particles with momentum between p and $p+dp$. The quantities F_x and $\langle\Delta_6^2\rangle$, which determine the momentum changes enforced by the random radiation, are given in Eqs. (29) and (53). We note that the Fokker-Planck equation (56) is linear in the oscillator damping constant Γ because F_x and $\langle\Delta_6^2\rangle$ are linear in Γ. Thus the equilibrium distribution is unaffected by how small the interaction between the oscillator and the radiation is, provided the interaction does not completely vanish.

The momentum distribution $P(p)$ is given on the infinite interval $-\infty<p<\infty$. In some cases it is convenient to give the velocity distribution $\mathcal{P}(\beta)$ on the finite interval $-1<\beta<1$, where $\mathcal{P}(\beta)d\beta$ is the number of particles with velocities between β and $\beta+d\beta$, where $\beta=v/c$. The connection between $P(p)$ and $\mathcal{P}(\beta)$ is derived from the relationship between the momentum and the velocity:

$$p=Mc\gamma\beta,\quad \gamma=(1-\beta^2)^{-1/2}\,. \tag{57}$$

It follows from (57) that

$$dp=Mc\gamma^3d\beta\,, \tag{58}$$

and thus the equality

$$P(p)dp=\mathcal{P}(\beta)d\beta$$

implies

$$P(p)=\mathcal{P}(\beta)/Mc\gamma^3\,. \tag{59}$$

The Fokker-Planck equation (56) for the momentum distribution is a first-order differential equation which can be solved directly as

$$P(p)=\text{const}\,\frac{\langle\Delta_6^2(0)\rangle}{\langle\Delta_6^2(\beta)\rangle}\exp\left(\int_0^p dp'\,\frac{2F_x(\beta')\tau}{\langle\Delta_6^2(\beta')\rangle}\right), \tag{60}$$

with the velocity β' appearing in $F_x(\beta')$ and $\langle\Delta_6^2(\beta')\rangle$ related to the momentum p' by the usual relations (57). The velocity distribution $\mathcal{P}(\beta)$ follows directly from (59) and (60):

$$\mathcal{P}(\beta)=\text{const}\gamma^3\frac{\langle\Delta_6^2(0)\rangle}{\langle\Delta_6^2(\beta)\rangle}\times\exp\left(M\int_0^\beta d\beta'\,\frac{2c\gamma'^3F_x(\beta')\tau}{\langle\Delta_6^2(\beta')\rangle}\right). \tag{61}$$

In this case the mass dependence is exhibited clearly. The functions $F_x(\beta)$ and $\langle\Delta_6^2(\beta)\rangle$ depend only upon the velocity β and the spectrum $g(\omega)$; the particle mass M appears in $\mathcal{P}(\beta)$ as only a multiplicative factor in the exponential.

III. EQUILIBRIUM DISTRIBUTIONS

A. Rayleigh-Jeans law and nonrelativistic limit

At this point in our analysis we have established the Fokker-Planck equation for the equilibrium distributions of particle momenta; we need only specify the spectrum of random classical radiation, and we can immediately obtain the associated equilibrium particle distribution.

Our first example will be the familiar case of the Rayleigh-Jeans law of thermal radiation,

$$g_{RJ}(\omega)=kT\,, \tag{62}$$

corresponding to energy equipartition with an average energy $\frac{1}{2}kT$ per normal mode at an absolute temperature T. It is this spectrum which, within classical physics, is familiarly connected with the Boltzmann distribution on phase space. Now all of the published derivations[15] for the association between the Rayleigh-Jeans law and the Boltzmann distribution actually involve nonrelativistic particle mechanics. Hence we will also go to the nonrelativistic limit.

In this nonrelativistic case, the values for F_x and $\langle\Delta_6^2\rangle$ are those of Eqs. (30) and (55), which when substituted into the solution (61) for the Fokker-Planck equation (56), give for the Rayleigh-Jeans spectrum (62)

$$P_{RJ}(p)=\text{const}\,\frac{\langle\Delta_6^2(0)\rangle}{\langle\Delta_6^2(\beta)\rangle}\times\exp\left(\int_0^p dp'\,\frac{2[-(2\Gamma\omega_0^2/5c)\beta'kT]\tau}{(4\Gamma\omega_0^2/5c^2)(kT)^2\tau}\right)$$

$$=\text{const}\exp(-p^2/2MkT)\,, \tag{63}$$

where we have used the nonrelativistic connection between velocity and momentum,

$$p = Mv = Mc\beta. \tag{64}$$

This is exactly the anticipated Boltzmann distribution for nonrelativistic free particles.

$$\begin{aligned} F_x &= \frac{3}{8}\frac{\Gamma\omega_0^3}{c}\int_{-1}^{1} dX\, X(1+X^2)\,\frac{kT}{\omega_0\gamma(1+\beta X)} \\ &= \frac{3}{8}\frac{\Gamma\omega_0^2}{c\gamma}kT\left[\frac{2}{3\beta}+\frac{2}{\beta}\left(1+\frac{1}{\beta^2}\right)-\frac{1}{\beta^2}\left(1+\frac{1}{\beta^2}\right)\ln\left(\frac{1+\beta}{1-\beta}\right)\right], \end{aligned} \tag{65}$$

$$\begin{aligned} \langle\Delta_6^2\rangle &= \gamma\frac{9}{32}\frac{\Gamma\omega_0^4}{c^2}\tau\int_{-1}^{1} dX\,\frac{X^2(1+X^2)kT}{\omega_0\gamma(1+\beta X)}\int_{-1}^{1} dY\,\frac{(1+Y^2)kT}{\omega_0\gamma(1+\beta Y)} \\ &= \frac{9}{32}\frac{\Gamma\omega_0^2}{c^2\gamma}\tau(kT)^2\left[\frac{-2}{\beta^2}+\frac{1}{\beta}\left(1+\frac{1}{\beta^2}\right)\ln\left(\frac{1+\beta}{1-\beta}\right)\right] \\ &\quad\times\left[-\frac{2}{3\beta^2}-\frac{2}{\beta^2}\left(1+\frac{1}{\beta^2}\right)+\frac{1}{\beta^3}\left(1+\frac{1}{\beta^2}\right)\ln\left(\frac{1+\beta}{1-\beta}\right)\right]. \end{aligned} \tag{66}$$

If these expressions for F_x and $\langle\Delta_6^2\rangle$ are substituted into the solution (60) of the Fokker-Planck equation, the result seems quite complicated. Some physicists anticipate that the particle distribution should be the Boltzmann distribution for relativistic free particles.[16] They argue that the textbooks connect classical Boltzmann statistics and the Rayleigh-Jeans law for thermal radiation; hence for relativistic particles the Boltzmann distribution for a relativistic particle energy is needed. However, this will not do. If expressions (65) and (66) are substituted into the Fokker-Planck equation (56), it is clear that the Boltzmann distribution

$$P_B(p) = \text{const}\exp[-(p^2c^2 + M^2c^4)^{1/2}/kT] \tag{67}$$

for relativistic free particles is not a solution of the equation. There is an inconsistency within classical electrodynamics between the Rayleigh-Jeans law for thermal radiation and the Boltzmann distribution for relativistic free particles.

In Fig. 1 we plot the results of computer evaluations for the velocity distributions $\mathcal{P}(\beta) = Mc\gamma^3 P(p)$ for both the Boltzmann distribution (67) and the distributions (61), (65), and (66) enforced by the Rayleigh-Jeans law. The distribution is symmetric between positive and negative velocities, and is independent of the oscillator frequency ω_0. The distributions are normalized to $\mathcal{P}(\beta) = 1$ at

B. Rayleigh-Jeans law and relativistic mechanics

Next we consider the equilibrium particle distribution for the situation of relativistic particle mechanics. The use of relativistic mechanics is, of course, the rigorously correct choice within classical physics, since it consistently matches the relativistic content of the Maxwell equations for electromagnetic fields. In this case we find from equations (29), (53), and (62) that

$\beta = 0$. The temperatures T are given in units of Mc^2/k where k is Boltzmann's constant. It is clear that the Rayleigh-Jeans law leads to the Boltzmann distribution at low temperatures where the velocities are nonrelativistic; indeed, the

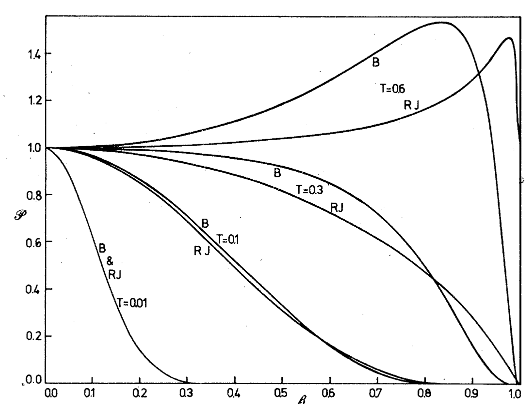

FIG. 1. Particle distributions for the Rayleigh-Jeans spectrum. The curves labeled RJ give the equilibrium velocity distribution $\mathcal{P}(\beta)$ for particles in the Rayleigh-Jeans spectrum of thermal radiation at temperature T. The Boltzmann distribution [Eqs. (59) and (67)] for relativistic free particles is given for comparison in the curves labeled B. Curves are normalized to $\mathcal{P}(\beta) = 1$ at $\beta = 0$, and the temperature is given in units of Mc^2/k, where Mc^2 is the particle rest energy and k is Boltzmann's constant.

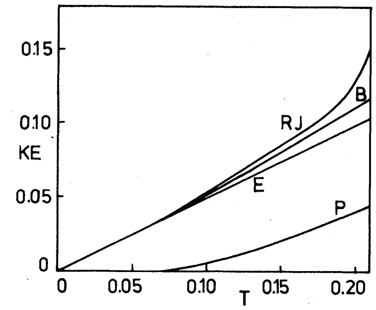

FIG. 2. Average kinetic energy per particle. The average kinetic energy KE per particle is given in units of Mc^2, the temperature T in units of Mc^2/k, and the frequency ω_0 in units of $Mc^2/\frac{1}{2}\hbar$. Only curve P for the Planck spectrum depends upon the choice of oscillator frequency, taken here as $\omega_0 = 0.1$. The straight line labeled E gives the equipartition value for the average kinetic energy per particle, KE$= \frac{1}{2}kT$. Curve B gives the average kinetic energy per particle for the Boltzmann distribution (67). Curves RJ and P give the average of the distribution (61) when substituting the Rayleigh-Jeans and Planck spectral distributions (62) and (68), respectively.

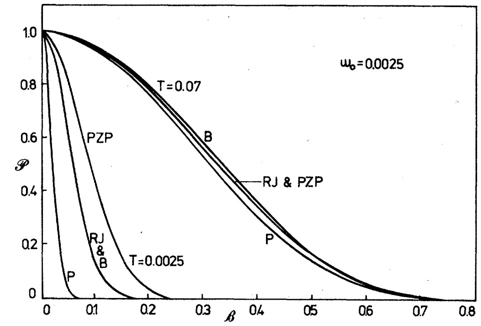

FIG. 3. Particle distributions for various radiation laws. The curves give the particle velocity distributions $\mathcal{P}(\beta)$ for the Boltzmann distributions (59) and (67), and for the distributions (61) when various radiation spectra (62), (68), and (75) are present. Curve B corresponds to the Boltzmann distribution. RJ labels the curve for the Rayleigh-Jeans spectrum (62), P the Planck spectrum (68), and PZP the Planck spectrum with zero-point radiation (75). The choice of frequency $\omega_0 = 0.0025$ affects curves P and PZP, but not B and RJ. The three curves at the left-hand side are for temperature $T = 0.0025$ and the three on the right-hand side are for $T = 0.07$. The normalization and choice of units is as in Figs. 1 and 2.

curves at $T = 0.01$ are indistinguishable in the figure. However, at high temperatures involving relativistic energies there is an increasingly large departure between the distributions. [The positive slopes seen for small β when $T = 0.6$ in Fig. 1 arise from the use of the distribution $\mathcal{P}(\beta)$ on velocity space with the associated factor of γ^3 in (59). The increase does not appear in a phase-space distribution.]

In Fig. 2 we find the average particle kinetic energy predicted by the Boltzmann distribution for relativistic free particles and by the Fokker-Planck results (29), (53), and (61) for the Rayleigh-Jeans law (62). The kinetic energy and temperature are given as fractions of the particle rest-mass energy. Thus the average particle kinetic energy is given in units of Mc^2 and the temperature in units of Mc^2/k. At low temperatures where the average kinetic energy is far below the particle rest energy Mc^2, the kinetic energy becomes the equipartition value $\frac{1}{2}kT$ for a free particle given in curve E. However, at higher temperatures the Boltzmann distribution for relativistic free particles increases[17] above the equipartition value as seen in curve B, while the average kinetic energy enforced by the Rayleigh-Jeans distribution increases enormously as seen in curve RJ. The average energy values reflect the departures seen in Fig. 1 where the Boltzmann distribution has a smaller number of particles at high velocity than does the distribution due to the Rayleigh-Jeans spectrum.

C. Planck spectrum without zero-point radiation

The Planck spectrum without zero-point radiation corresponds to an energy per normal mode

$$g_P(\omega) = \hbar\omega/[\exp(\hbar\omega/kT) - 1]. \tag{68}$$

This spectrum can be substituted into Eqs. (29), (53), and (61) to give the associated equilibrium distribution $\mathcal{P}(\beta)$ for classical particles. Some results obtained from computer calculations are given in Figs. 2 and 3.

At very low temperatures $kT \ll \hbar\omega_0$, the Planck spectrum without zero-point radiation becomes the Wien spectrum,

$$g_W(\omega) = \hbar\omega \exp(-\hbar\omega/kT) \tag{69}$$

which is much smaller than the Rayleigh-Jeans law, and hence at low temperatures the associated particle distribution $\mathcal{P}_P(\beta)$ falls well below the Boltzmann distribution $\mathcal{P}_B(\beta)$ appropriate for nonrelativistic velocities. Just this situation is seen at $T = 0.0025$ in Fig. 3.

In the high-temperature limit $kT \gg \hbar\omega_0$, the Planck spectrum without zero-point radiation comes close to, but still below, the Rayleigh-Jeans distribution $g_{RJ}(\omega) = kT$, since (68) becomes

$$g_P(\omega) \cong kT - \tfrac{1}{2}\hbar\omega. \tag{70}$$

The curves in Fig. 3 for $T = 0.07$ correspond to this situation and show the equilibrium distribution $\mathcal{P}_P(\beta)$ for the Planck spectrum near, but still below, $\mathcal{P}_{RJ}(\beta)$ for the Rayleigh-Jeans spectrum.

In Fig. 2, curve P shows the average kinetic energy for particles in the Planck radiation spectrum. We note that the average kinetic energy at low temperature lies far below the equipartition value, corresponding to the small amount of radiation (69) at low temperatures interacting with the oscillator at natural frequency ω_0. The choice of ω_0 in Fig. 2 is $\omega_0 = 0.1$, in units of $Mc^2/\frac{1}{2}\hbar$.

D. Zero-point radiation spectrum

If the radiation spectrum is that of classical zero-point radiation

$$g_{ZP}(\omega) = \tfrac{1}{2}\hbar\omega\,, \tag{71}$$

then the average force F_x in (29) vanishes, and the mean-square impulse delivered to the oscillator is

$$\langle\Delta_0^2\rangle = \gamma 4\Gamma\omega_0^4\tau/5c^2\,. \tag{72}$$

Substituting these values into the solution (60) for the Fokker-Planck equation, we have the equilibrium distribution of momenta

$$P(p) = \text{const}\gamma^{-1} = \text{const}\,E^{-1}\,, \tag{73}$$

or, from (61), the equilibrium distribution of velocities

$$\mathcal{P}(\beta) = \text{const}\,\gamma^2. \tag{74}$$

These distributions are Lorentz-invariant, as we would expect since the spectrum of zero-point radiation itself is Lorentz-invariant.[11] Thus any observer moving with constant velocity along the x axis, which is the axis of constraint for our particles, will see the same momentum distribution of particles independent of the observer's velocity. If there are $P(p)dp = \text{const}\,dp/E$ particles between p and $p+dp$ in the lab frame, then an observer moving along the x axis with velocity V sees this same number of particles in the interval

$$dp^* = \gamma(dp - V\,dE/c^2) = \gamma(1 - Vp/E)dp$$

at an energy $E^* = \gamma(E - Vp)$, where $\gamma = (1 - V^2/c^2)^{-1/2}$. Hence the moving observer reports

$$P^*(p^*)dp^* = P(p)dp = \text{const}\,dp/E = \text{const}\,dp^*/E^*$$

particles, corresponding to a distribution $P^*(p^*) = \text{const}/E^*$ which is identical in form to the original distribution in the lab frame. The distribution is Lorentz invariant.

The equilibrium velocity distribution of (74) is plotted in Fig. 4 as the curve labeled $T=0$ corresponding to zero temperature, normalized to $\mathcal{P}(\beta) = 1$ at $\beta = 0$. It is clear that the curve involves an infinite number of particles and infinite total energy. Also, the average kinetic energy per particle is infinite, so that we cannot enter the value at $T=0$ in Fig. 2.

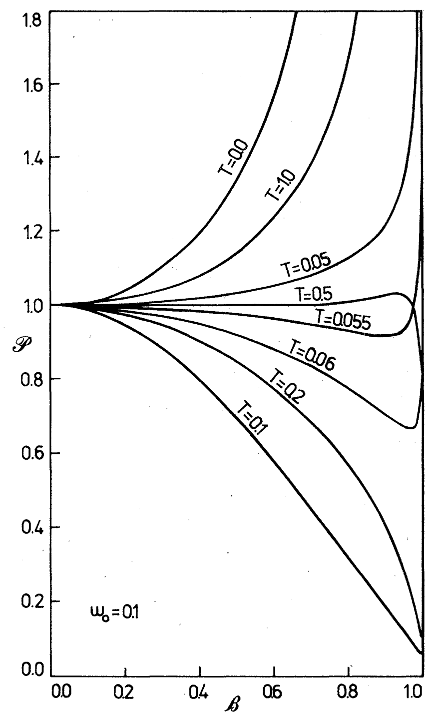

FIG. 4. Particle distributions for the Planck law with zero-point radiation. Curves are normalized to $\mathcal{P}_{PZP}(\beta) = 1$ when $\beta = 0$. Temperatures are measured in units of Mc^2/k and the frequency $\omega_0 = 0.1$ is in units $Mc^2/\frac{1}{2}\hbar$, where Mc^2 is the particle rest energy. All equilibrium distributions show divergent tails at high velocities. The curve for $T=0.0$ is given by $\mathcal{P}_{PZP}(\beta) = \gamma^2$. High- and low-temperature curves occupy the same region of the diagram but have different shapes.

E. Planck spectrum with zero-point radiation

Experimental measurements of thermal radiation, random radiation in excess of that present at zero temperature, are in good agreement with the Planck spectrum (68). However, there is also strong experimental evidence[18] which suggests the presence of zero-point radiation. Thus it may well be that the spectrum of random classical radiation which describes nature most closely is Planck's spectrum with zero-point radiation,

$$\begin{aligned} g_{PZP}(\omega) &= \hbar\omega/[\exp(\hbar\omega/kT) - 1] + \tfrac{1}{2}\hbar\omega \\ &= \tfrac{1}{2}\hbar\omega\coth(\hbar\omega/2kT)\,. \end{aligned} \tag{75}$$

This spectrum leads to quite curious behavior for the equilibrium velocity distribution of free particles.

Figure 4 gives the graphs of the computer results when the Planck spectrum with zero-point radiation (75) is substituted into Eqs. (29) and (53) for F_x and $\langle\Delta_\delta^2\rangle$, and then these are inserted into the result (61) for the Fokker-Planck equation. The graphs are normalized so that $\mathcal{P}(\beta)=1$ at $\beta=0$, and are given for a large value, $\omega_0=0.1$, of the oscillator frequency ω_0, in order to show clearly the unusual aspects of the distribution.

All of the graphs diverge at a high velocity. At zero temperature, $T=0.0$, we have the Lorentz-invariant distribution $\mathcal{P}(\beta)=\gamma^2$. At temperatures slightly above zero, the distribution becomes flatter before increasing into the high-velocity tail. This is found in the curves labeled $T=0.05$ and $T=0.055$ in Fig. 4. For still higher temperatures, seen in the curves $T=0.06$ and $T=0.1$, the low-velocity distribution falls more sharply and begins to approximate the shape of the Boltzmann distribution before rising at a high velocity. However, the curve at $T=0.1$ corresponds to a limiting situation; at higher temperatures the curves lie above that for $T=0.1$. At very high temperatures the momentum distribution in phase space gets quite flat at low momentum, and hence the velocity distribution $\mathcal{P}(\beta)\propto\gamma^3P(p)$ increases as γ^3 for low velocities. This rise is seen in curves $T=0.5$ and $T=1.0$ in Fig. 4.

If we choose a smaller frequency ω_0, it becomes clearer that the low-velocity distribution goes over to the Boltmann distribution for temperatures such that $\hbar\omega_0\ll kT\ll Mc^2$. This situation is found in curves PZP of Fig. 3, which correspond to the Planck spectrum with zero-point radiation for $\omega_0=0.0025$. If $\hbar\omega_0\ll kT\ll Mc^2$, the low-velocity behavior is separated from the high-velocity tail by a region where $\mathcal{P}(\beta)$ is extremely small, the region corresponding to the Boltzmann exponential falloff. In Fig. 3, the probability density drops below 10^{-36}, the smallest value carried by the computer, before going over to the divergent tail.

A clearer idea of the high-velocity asymptotic behavior for the velocity distribution $\mathcal{P}_{\mathrm{PZP}}(\beta)$ can be obtained as follows. The crucial step involves showing that the quantity

$$\int d\beta'\, 2c\gamma'^3F_x\tau/\langle\Delta_\delta^2\rangle$$

appearing in the exponential of Eq. (61) is finite for the upper limit of integration extended to $\beta=1$. The integrands for the two integrals needed for $\langle\Delta_\delta^2\rangle$ in Eq. (53) are both positive, and for large β will be dominated by the zero-point radiation at large frequency in g_{PZP}. Thus we can replace g_{PZP} in (53) by g_{ZP} and so obtain for large β,

$$\langle\Delta_\delta^2\rangle\sim\gamma4\Gamma\omega_0^4(\tfrac{1}{2}\hbar)^2/5c^2\,. \tag{76}$$

The integrand for the function F_x in (29) is quite different. In this case the integrand receives both positive and negative contributions depending upon whether $X>0$ or $X<0$, and the integral vanishes if g is linear in frequency. For large values of β, the integral is dominated by the contribution for $X\to-1$, where the denominator $\omega_0\gamma(1+\beta X)$ is small and the numerator $g_{\mathrm{PZP}}(\omega_0\gamma(1+\beta X))$ involves the Rayleigh-Jeans limit kT holding at small frequencies. Thus F_x is dominated by the integral

$$F_x\sim\frac{3}{8}\,\frac{\Gamma\omega_0^3}{c}\int_{-1}^{0}dX\,\frac{X(1+X^2)kT}{\omega_0\gamma(1+\beta X)}\,, \tag{77}$$

where we have taken the upper limit $x=0$. This involves the same integrand that appears in the case of the Rayleigh-Jeans law, and so has the same behavior at large β as Eq. (65),

$$F_x\sim-\tfrac{3}{8}(\Gamma\omega_0^2/c\gamma)kT2\ln[2/(1-\beta)]\,. \tag{78}$$

Thus at large β the integrand in (61) for $\mathcal{P}(\beta)$ involves

$$\begin{aligned}\int^1 d\beta'\,&\frac{2c\gamma'^3(3\Gamma\omega_0^2/8c\gamma')kT2\ln(1-\beta)}{(\gamma'4\Gamma\omega_0^4/5c^2)(\frac{1}{2}\hbar)^2}\\ &\sim\text{const}\int^1 d\beta'\,\gamma'\ln(1-\beta')\\ &\sim\text{const}\int^1 d\beta'\,(1-\beta')^{-1/2}\ln(1-\beta')\,.\end{aligned} \tag{79}$$

Substituting $u^2=1-\beta'$, we see that the integral becomes

$$\int^0 du\,\ln u=(u\ln u-u)\big|^{u=0}\,,$$

which is finite. Thus from (61) and (76) we find that the velocity distribution $\mathcal{P}(\beta)$ normalized to give $\mathcal{P}(\beta)=1$ at $\beta=0$ behaves for large β as

$$\begin{aligned}\mathcal{P}(\beta)&=\gamma^2\exp\left(M\int_0^1 d\beta'\,\frac{2c\gamma'^3F_x(\beta')\tau}{\langle\Delta_\delta^2(\beta')\rangle}\right)\\ &=\text{const}\,\gamma^2\,.\end{aligned} \tag{80}$$

This is just the Lorentz-invariant distribution (74).

From equations (29), (53), (75), and (80), we see that the value of β where the Lorentz-invariant tail becomes evident depends upon the ratio $kT/\hbar\omega$, starting with $\beta=0$ for $T=0$ and moving to higher β as T becomes larger. The value of the constant multiplying the tail distribution depends upon the particle mass M, and, since F_x is negative, becomes exponentially smaller as M becomes larger. It is for this reason that in Fig. 4, where we wished to illustrate the high-velocity behavior of the distributions, we used a small value of M or, equivalently, large values of ω_0 and T relative to the value of M. In the reverse situation involving large values of M, or small values of ω_0 and T, such as in Fig. 3, the divergent tail would be lost at the $\beta = 1$ edge of the diagram.

In summary we conclude the following. For the Planck spectrum with zero-point radiation, the equilibrium velocity distribution for free particles evolves smoothly from the zero-point distribution. In every case, the equilibrium velocity distribution involves an infinite number of particles, an infinite total energy, and an infinite average kinetic energy per particle. No finite number of free particles can be in velocity equilibrium with thermal radiation at any finite temperature. If a finite number of free particles start at a finite velocity, they will gradually diffuse to ever-higher velocities. At high velocity, a particle sees the thermal radiation Doppler-shifted to frequencies which do not interact significantly with the internal oscillator at a frequency ω_0; it is the Lorentz-invariant zero-point radiation which interacts with the oscillator and pushes the particle toward a Lorentz-invariant distribution at high velocities. We conclude that particle equilibrium in the presence of the Planck radiation spectrum including zero-point radiation is not possible for a free particle, but rather requires particle binding to eliminate the high-velocity tail on the distribution.[19]

IV. CLOSING SUMMARY

Within classical physics, the equilibrium distribution for particles at a given temperature and the distribution of random radiation at a given temperature arise from very different lines of argument. The distribution of particle velocities is usually found from statistical mechanics in which electromagnetic interactions are ignored. Thermal radiation is usually considered as a result derived from previous results for particle equilibrium. In the present paper we reverse this last procedure and derive the distribution of particle velocities for free particles when we assume various results for the equilibrium spectrum of classical thermal radiation.

Our investigation starts from the model proposed by Einstein and Hopf in 1911, but extends their work to the realm of relativistic particle velocities. The model envisages a massive free particle which contains an electric dipole oscillator interacting with the random classical radiation. The radiation delivers random impulses to the oscillator which cause it to execute a Brownian motion. Using a Fokker-Planck equation in the particle momentum, we obtain the equilibrium distribution of the particle momentum imposed by the radiation spectrum. Finally we solve the Fokker-Planck equation to obtain the actual momentum distribution.

Our results for the equilibrium distributions yields some expected and some surprising results. We find that the Rayleigh-Jeans law leads to the Boltzmann distribution for nonrelativistic free particles; however, the Rayleigh-Jeans law does not lead to the Boltzmann distribution for relativistic free particles. Here relativity interjects a new element into the problem of thermal equilibrium of particles and radiation within classical theory.

For the zero-point radiation spectrum, we find the expected Lorentz-invariant particle distribution; however, for the Planck spectrum with zero-point radiation, this Lorentz-invariant distribution still appears as the asymptotic particle distribution at high velocities. Hence if zero-point radiation is present, a free particle is never in equilibrium with thermal radiation. Only if the particle is bound can it be prevented from diffusing gradually up to velocities ever closer to the speed of light.

---

[1]A. Einstein and L. Hopf, Ann. Phys.(Leipz.) 33, 1105 (1910).
[2]E. A. Milne, Proc. Cambridge Philos. Soc. 23, 465 (1926).
[3]T. H. Boyer, Phys. Rev. 182, 1374 (1969).
[4]See, for example, A. P. French, *Special Relativity* (Norton, New York, 1968), p. 237.
[5]T. H. Boyer, Phys. Rev. D 11, 790 (1975).
[6]J. D. Jackson, *Classical Electrodynamics*, 2nd ed. (Wiley, New York, 1975), p. 552.
[7]See Ref. 6, p. 516.
[8]See Ref. 6, p. 521.
[9]T. H. Boyer, Phys. Rev. A 6, 314 (1972).
[10]T. H. Boyer, Phys. Rev. A 18, 1228 (1978).
[11]T. W. Marshall, Proc. Cambridge Philos. Soc. 61, 537 (1965); T. H. Boyer, Phys. Rev. 182, 1374 (1969).
[12]See Ref. 3, Eq. (51).
[13]See Ref. 3, Eq. (63).
[14]T. Reif, *Fundamentals of Statistical and Thermal Physics* (McGraw-Hill, New York, 1965), p. 579.
[15]See, for example, M. Born, *Atomic Physics*, 7th ed. (Hafner, New York, 1966), p. 254; and T. H. Boyer, Phys. Rev. D 13, 2832 (1976); Phys. Rev. A 18, 1228 (1978).
[16]The Boltzmann distribution for relativistic free particles can be derived from relativistic collisions between the particles. See S. R. de Groot, in *Proceedings of the International Symposium "100 Years Boltzmann Equation," Vienna, 1972*, edited by E. G. D. Cohen and W. Thirring (Springer, Berlin, 1973); Acta

Phys. Austriaca Suppl. 10, 529 (1973). de Groot obtains the relativistic ideal-gas distribution of F. Jüttner [Ann. Phys. (Leipz.) 34, 856 (1911)].

[17]See F. Jüttner, Ann. Phys. (Leipz.) 34, 856 (1911).

[18]See the information presented in Ref. 5.

[19]This observation is very similar to that of Sec. VI in Ref. 3 leading to the derivation of the blackbody radiation spectrum.